

PAPER • OPEN ACCESS

Modification of the atomic structure of metallic materials after strong external exposures

To cite this article: V A Ivchenko 2018 *IOP Conf. Ser.: Mater. Sci. Eng.* **447** 012012

View the [article online](#) for updates and enhancements.

You may also like

- [Templating ultra-small manganese isomers with preference for adsorption sites and narrow distribution tuned by different moiré periodicities of monolayer graphene on Ru\(0001\)](#)
Ke Wu, Hanjie Zhang, Yao Wang et al.
- [Organ doses from environmental exposures calculated using voxel phantoms of adults and children](#)
Nina Petoussi-Henss, H Schlattl, M Zankl et al.
- [A new method of estimation of dose conversion coefficients for aquatic biota](#)
Yang Li, Jianguo Li, Huijuan Wang et al.

PRIME
PACIFIC RIM MEETING
ON ELECTROCHEMICAL
AND SOLID STATE SCIENCE

HONOLULU, HI
Oct 6–11, 2024

Abstract submission deadline:
April 12, 2024

Learn more and submit!

Joint Meeting of
The Electrochemical Society
•
The Electrochemical Society of Japan
•
Korea Electrochemical Society

Modification of the atomic structure of metallic materials after strong external exposures

V A Ivchenko

Yeltsin Ural Federal University, 19 Mira st. Yekaterinburg, 620002, Russia
Institute of Electrophysics, Ural Branch, Russian Academy of Sciences, 106
Amundsen st., 620016, Yekaterinburg, Russia

e-mail: ivchenko2008@mail.ru

Abstract. The paper presents the application of direct methods (field ion microscopy and atom probe techniques) to study the modification of the crystal structure of various materials at the atomic spatial level after strong external exposures. The effects of amorphization of subsurface volumes of alloys, deformation effects in pure metals, and structural phase transformations in subsurface volumes of solid solutions were detected during radiation exposure to charged particle beams with an energy of 20 keV. The original results show the possibility of three-dimensional reconstruction of the elemental composition of the materials investigated with atomic resolution to study the modification of the atomic structure. It is established that the nature of the crystalline structure of the boundary region of planar defects directly depends on the type of external influence. Experimental data on the elemental composition of interphase interfaces in mechanically alloyed compounds and doped alloys have been obtained. It is established that the width of the boundary regions at the metal interfaces varies within 0.8–1.5 nm, depending on the type of intensive external action to which they were subjected.

1. Introduction

Among the most efficient and advanced methods to study conducting and semiconducting materials, using which the lattice of solids can be directly studied with the atomic spatial resolution, are field ion microscopy (FIM) and various modifications of atom probes of a field ion microscope.

The objective of this paper is to demonstrate the efficient use of atom probe methods for studying nanostructured states arising in the bulk of metals and alloys during modification of the atomic structure of various materials by strong external exposures. It is shown that, along with the lattice distortions typical of thermo- mechanical, thermal, strong deformational, and other perturbations (dot, linear, dislocation, and other lattice defects), the studied materials contain such radiation defects as vacancy clusters, amorphized regions, and nano segregations of atoms of one of the components in ordered alloys. The microscope field size (~100 nm) and analysis of the sample volume by controlled layer by layer evaporation of the surface atoms make it possible to determine whether the material under study is nanostructured or not. The possibility of studying the sample in a volume down to micron sizes makes it possible to obtain macro scale experimental data.

FIM is the only microscopy technique capable of providing direct observation of individual atoms as elements composing the structure of a sample during an ordinary experiment. The use of FIM makes it possible to select an individual atom in the image for mass spectrometric identification (atom probe FIM methods), to perform in situ experiments with individual atoms deposited on the surface,



and to reconstruct the structural and chemical compositions in the sample volume by controlled layer by layer removal of surface atoms by an electric field at cryogenic temperatures. Exactly the latter situation distinguishes direct FIM methods from other structurally sensitive ones with atomic resolution, but being indirect methods of microscopic study of materials.

2. Experimental

The samples to be studied were prepared as tip emitters with an apex curvature radius of 30–50 nm from materials preliminarily processed by various strong external exposures, i.e., electrochemically polished wires or rods.

The objects of interaction with accelerated beams of gas ions ($E = 20$ keV, implantation dose $D = 10^{13}$ – 10^{18} ion/cm², and current density $j = 100$ – 340 μ A/cm²) were various metal materials. Field emitters certified for ion implantation were characterized by the atomically smooth surface of the apex prepared in situ by field evaporation of surface atoms.

Figure 1 shows the ion image of Pt after certification. On the one hand, the micropattern represents the contrast of the tip end surface from atoms at the edges of the step; on the other hand, it reflects the stereographic projection of the crystal under study. Circular contour lines in the ion image are the edges of the corresponding sets of crystallographic planes of certain directions. Adjacent rings (from any set of concentric rings) represent images of parallel atomic layers. The distance between the rings corresponds to the interplanar distance for a given crystallographic direction. In terms of the ion microscopic image, this distance also refers to the lattice step height. The rings themselves in the ion microscopic image, as a rule, consist of isolated bright dots which are images of surface atoms arranged at atomic sites in step edges.

Materials such as Cu₈₀Co₂₀ were mechanical alloyed by high purity (99.9%) Cu and Co powders with particle sizes of ~ 50 μ m. The powders were treated in a centrifugal planetary mill in an argon atmosphere at room temperature for 20 hours. The ratio of steel balls of the mill to powder particles was 1: 25. After mechanical alloying, the powders were compacted into pellets by compression shear at 500 MPa. Some pellets were annealed at 400 °C for 2 hours. Work pieces for future pins were rods ($\sim 0.2 \times 0.2 \times 10$ mm³ in volume) cut from thermally treated pellets by spark cutting. Tomographic atom probe (TAP) studies were performed with the ratio of the pulse voltage to the dc voltage of 20% and the repetition rate of 775 Hz in high vacuum (1×10^{-8} Pa). The sample temperature during measurements was 60–80 K.

3. Results and considerations

The objects of interaction with accelerated beams of gas ions were pure metals (Ir), atomically ordered alloys (Cu₃Au), and solid solutions (50Pd₃₀Cu₂₀Ag), the decomposition of which leads to atomically ordered phase separation [1-7].

Using the FIM method, the effect of partial amorphization in the subsurface volume of atomically ordered alloys was detected due to the implantation of positive argon ions accelerated to 20 keV ($D = 10^{18}$ ion/cm² and $j = 200$ μ A/cm²) [6]. Partial amorphization was observed at distances of at least 90 nm from the irradiated surface of materials. In the experiment, only the beam current density varied; the implantation energy and dose did not change ($E = 20$ keV, $D = 10^{18}$ ion/cm²). At $j = 275$ μ A/cm², a structural phase transition occurred in the entire volume of the material, which indicated that the sample was heated to the critical phase transformation temperature (~ 390 °C), and the cooling rate corresponded to the conditions of the transition to a disordered state.

Figure 2 shows the ion pattern of the irradiated platinum surface with the fluence of 10^{18} ions/cm².

It is obvious, that on the basis of the contrast of micro patterns of the atomically smooth platinum surface when analyzing the subsurface regions of the material during the controlled elimination of atomic layers, the phase state of the metal becomes almost amorphous with an increase in the fluence of up to 10^{18} ions/cm².

The proof of this is the structureless arrangement of atoms in the subsurface layers. The counterpart of the observed ion pattern corresponds to the ion pattern of amorphous materials obtained by ultrafast

cooling. In our estimation, the amorphization of the pure metal (Pt) occurs in the subsurface region at a depth of 12 nm from the irradiated surface.

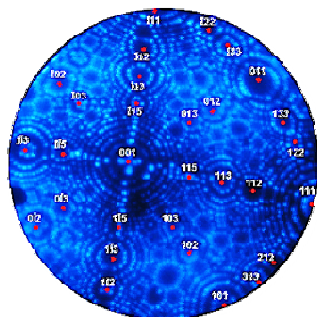


Figure 1. Neon image of Pt single crystal, $U = 10$ kV.

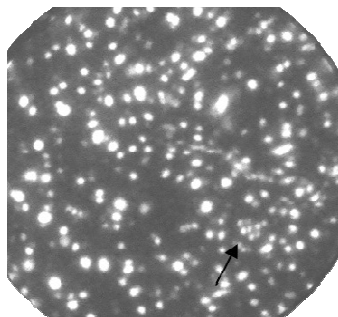


Figure 2. Ion pattern of Pt surface after irradiation by Ar^+ with $D = 10^{18}$ ions/cm² ($T = 300^\circ C$) (the arrow denotes the region of the crystalline state of the metal).

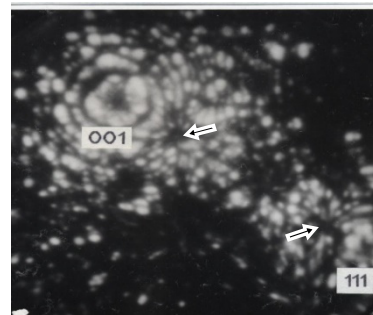


Figure 3. A region of ion contrast of ion-implanted PdCuAg after the removal of 14 atomic layers of the irradiated surface (arrows show ion contrast micropores).

The study of ion implanted PdCuAg detected a phase structural transition in its subsurface volume [4]. The size of the surface volume in which the structural phase transformation was detected was estimated as a function of the beam current density. In the subsurface volume, vacancy clusters (micropores) were detected (figure 3), and their sizes and shape were estimated. Micropores were shaped as ellipsoids with a height of 4–25 nm and a diameter of 3–12 nm. The volume fraction of micropores monotonically decreases with distance from the irradiated surface.

The study of mechanically deformed iridium samples revealed a high density of point, linear, and volume structural defects. A comparative analysis of planar defects [1], observed in pre-deformed (~90%) and irradiated iridium, showed a significant difference between their structures. Mechanically deformed iridium consisted of grains with sizes within 20–30 nm, the bodies of which were almost free of structural defects. In contrast, the ion irradiated metal ($E = 20$ keV, $D = 10^{18}$ ion/cm², $j = 300$ $\mu A/cm^2$) exhibited a sub-block microstructure with a characteristic size of ~3–5 nm, block misorientation within $0.5^\circ - 1^\circ$, and various defects in the bodies of blocks.

The width of the boundary regions at the interfaces in the samples upon various external actions was, similarly to the heat treated metals and alloys, of the order of the interatomic distances.

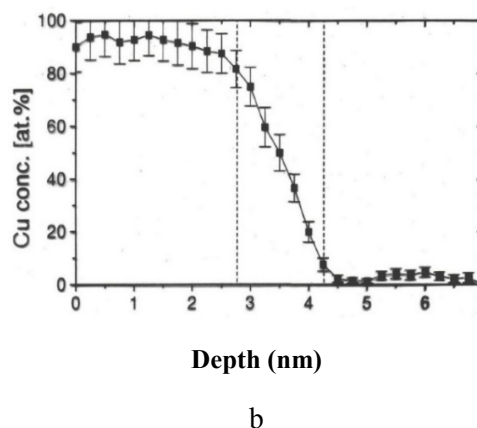
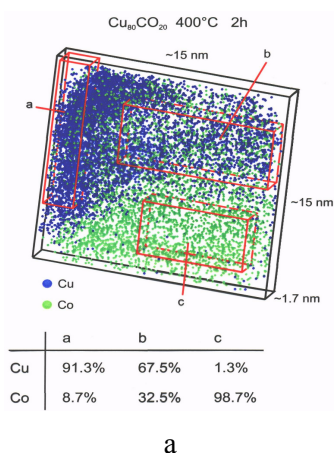


Figure 4. (a) 3D elemental map of the mechanically alloyed Cu₈₀Co₂₀ compound (upon annealing at 400 °C for 2h) as reconstructed by the TAP data; (b) interphase boundary width of the mechanically alloyed Cu₈₀Co₂₀ compound upon 2 h of annealing.

The width of the boundary region changes significantly in the case of materials obtained by mechanical alloying (figure 4) [8]. Figure 4a shows a three-dimensional (3D) reconstruction of the

elemental map of the mechanically alloyed Cu₈₀Co₂₀ compound. The determination of the composition of the annealed material revealed three regions with different concentrations of cobalt: (a) a region containing 8.7 at.% Co, (b) an intermediate region containing 32.5 at.% Co, and (c) a region with high concentration of Co and only 1.3 at.% Cu. All these regions exhibit interphase boundaries with an effective width of about 1.5 nm (figure 4b). The plot in figure 4b shows a variation of copper content in the boundary regions of the interphase interfaces.

The FIM study of nickel samples clearly revealed the boundaries of ultradisperse blocks, which constitute the microstructure of individual grains [9]. The dimensions of blocks, estimated both on the surface FIM image and in the course of the controlled sequential removal of the surface atomic layers, varied from 1 to 10 nm. The widths of the boundary regions were of the order of the interatomic distance. In the first approximation, the obtained data are identical to the results of studying the atomic structure in submicrocrystalline (SMC) tungsten (with an average grain size of ~100 nm) upon severe plastic deformation ($\epsilon \approx 7$) [10]. The analysis of the FIM images of an SMC tungsten surface region with a grain boundary showed that its width was about 0.6–0.8 nm. It should be noted that the width of the boundary in the initial coarse-grained tungsten was 0.3–0.4 nm [9]. In addition, the use of field electron microscopy (FEM) and electron spectroscopy techniques revealed significant differences between the electron energy distributions in SMC and coarse grained tungsten [10].

4. Conclusions

Thus, the application of direct methods for studying the crystal structure of various materials at the atomic spatial level (field ion microscopy and atom probe FIM methods) after various intensive external exposures was demonstrated. For example, the effects of amorphization of subsurface volumes of alloys, deformation effects in pure metals, and structural phase transformations in subsurface volumes of solid solutions were detected during the radiation exposure to the charged particle beams with an energy of 20 keV. It is established that the nature of the crystalline structure of metal interfaces significantly depends of the type of external actions and eventually determines the physical (in particular, mechanical) properties of materials.

Experimental data on the elemental composition of interphase interfaces in mechanically alloyed compounds have been obtained. It is established that the width of the boundary regions at the metal interfaces varies within 0.8–1.5 nm, depending on the type of the intensive external action to which they were subjected.

Acknowledgments

This work was supported by RFBR Grant No. 16-08-00615.

References

- [1] Ivchenko V A and Syutkin N N 1999 *Techn. Phys. Lett.* **25** 3 233
- [2] Bunkin A Yu, Gavrilov N V, Ivchenko V A, Kreindel, Y E, Kuznetsova L Yu and Syutkin N N 1990 *Fizika Metallov i Metallovedenie* **69** 171 (In Russian)
- [3] Bunkin A Yu Ivchenko V A, Kuznetsova L Yu and Syutkin N N 1990 *Fizika Metallov i Metallovedenie* **7** 111 (In Russian)
- [4] Ivchenko V A and Syutkin N N 1995 *Surf. Sci.* **87/88** 257
- [5] Ivchenko V A, Syutkin N N and Bunkin A Yu 1988 *J. Phys.* **49**–C6 379
- [6] Ivchenko V A, Syutkin N N and Kuznetsova L Yu 2000 *Techn. Phys. Lett.* **26** 541
- [7] Ivchenko V A, Ovchinnikov V V, Goloborodsky B Yu and Syutkin N N 1997 *Surf. Sci.* **384** 46
- [8] Ivchenko V, Wanderka N, Czubyko U, Naundorf V, Ermakov AYe, Uimin M A and Wollenberg H 2000 *Mater. Sci. Forum* **343/346** 709
- [9] Ivchenko V A, Efros B M, Popova E V, Efros N B, Loladze L V 2003 *Fizika i Tekhnika Vysokikh Davlenii* **13** 3 159 (In Russian)
- [10] Mulyukov R R, Yumaguzin Yu M, Ivchenko V A and Zubairov L R 2000 *JETP Lett.* **72** 5 257